MOLECULAR AND CELLULAR BIOLOGY, Jan. 2000, p. 684–696 Vol. 20, No. 2
0270-7306/00/$04.00+0

Caspase 3 Cleavage of the Ste20-Related Kinase SLK Releases and Activates an Apoptosis-Inducing Kinase Domain and an Actin-Disassembling Region

LUC A. SABOURIN,[1] PATRICK SEALE,[1,2] JULIAN WAGNER,[1] AND MICHAEL A. RUDNICKI[1]*

Institute for Molecular Biology and Biotechnology[1] and Department of Biology,[2] McMaster University, Hamilton, Ontario, Canada

Received 4 May 1999/Returned for modification 15 June 1999/Accepted 27 September 1999

We have demonstrated that a novel Ste20-related kinase, designated SLK, mediates apoptosis and actin stress fiber dissolution through distinct domains generated by caspase 3 cleavage. Overexpression of SLK in C2C12 myoblasts stimulated the disassembly of actin stress fibers and focal adhesions and induced apoptosis, as determined by annexin V binding and terminal deoxynucleotidyltransferase-mediated dUTP-biotin nick end labeling analysis. SLK was cleaved by caspase 3 in vitro and in vivo during c-Myc-, tumor necrosis factor alpha, and UV-induced apoptosis. Furthermore, cleavage of SLK released two domains with distinct activities: an activated N-terminal kinase domain that promoted apoptosis and cytoskeletal rearrangements and a C-terminus domain that disassembled actin stress fibers. Moreover, our analysis has identified a novel conserved region (termed the AT1-46 homology domain) that efficiently promotes stress fiber disassembly. Finally, transient transfection of SLK also activated the c-Jun N-terminal kinase signaling pathway. Our results suggest that caspase-activated SLK represents a novel effector of cytoskeletal remodeling and apoptosis.

Programmed cell death, or apoptosis, is a genetically controlled process triggered by various stimuli in different cells. External stimuli such as cytokines, UV irradiation, and numerous drugs induce an apoptotic response characterized by a series of morphological changes that include cytoplasmic shrinkage, membrane blebbing, chromatin condensation, DNA fragmentation, and the formation of apoptotic bodies (22, 44, 54). Several studies have revealed the catalytic activation of several kinases during apoptosis. For example, the c-Jun N-terminal kinase (JNK) pathway is activated in response to apoptotic triggers such as tumor necrosis factor alpha (TNF-α) and Fas ligand (57, 60, 62). In addition, activation of other kinases, such as ASK1, RIP, and ZIP kinases, stimulates apoptosis in cultured (16, 21, 53).

The induction of apoptosis involves a proteolytic activation of a cascade of a family of cysteine proteases called caspases. Aggregation of death receptors following ligand binding activates initiator caspases, which in turn activate downstream effector caspases through proteolytic processing (55). Caspases contribute to cell death by direct inactivation of negative regulators of apoptosis and by promoting the disassembly of cellular structures such as focal adhesion complexes (55). Although several caspase substrates such as nuclear lamins and poly-ADP ribose polymerase have been identified (55), little is known about the biological function of the cleavage products. However, recent studies have revealed that caspase-mediated cleavage of the serine/threonine kinase PAK2 ($p65^{PAK}$) generates a catalytically active fragment involved in regulating some of the morphological changes associated with apoptosis (28, 47). Caspases similarly cleave the Ste20-related kinase MST1 to release a catalytically active kinase domain that activates stress-activated protein kinases (SAPKs) as well as MKK6 and MKK7 (15, 27).

The small GTPase proteins of the Rho subfamily mediate various cellular processes such as growth and cytoskeleton reorganization through direct binding of the activated GTP-bound forms to downstream targets (56). RhoA is required for maintenance of actin stress fibers and focal adhesions in cultured cells. These activities have been shown to be mediated by several Rho-associated protein kinases such as ROKα, $p160^{ROCK}$, MRCKα, protein kinase N, and PRK2 (1, 2, 18, 29, 30, 36, 59). The Cdc42 GTPase promotes the formation of actin microspikes, whereas Rac1 activation induces the formation of lamellipodia or membrane ruffles. In addition to playing an important role in cellular morphology, the Rho family of GTPases regulates transcription through the JNK and p38 pathways (13). Mammalian targets of Cdc42 and Rac1 include the PAK family of protein kinases (56). Upon binding to activated Cdc42 or Rac1, PAK is activated and translocated to focal adhesion sites (32). Expression of constitutively active α-PAK causes the loss of focal adhesions and retraction of actin stress fibers to the periphery (32). In addition, PAK activation leads to stimulation of the SAPK and p38 kinase pathways (13).

We have cloned and characterized a murine Ste20-related kinase called SLK. Here we present biochemical evidence that apoptotic triggers induce proteolytic processing of SLK into an activated kinase domain and an actin stress fiber dissolution region. Our results suggest that caspase-mediated activation of SLK represents a novel effector of actin stress fiber disassembly and apoptosis.

MATERIALS AND METHODS

Cloning and sequence analysis. During the course of a two-hybrid screen for proteins interacting with a muscle-specific transactivator, several putative binding proteins were isolated. One clone contained a 1.6-kb partial cDNA insert that showed extensive homology to a human serine/threonine protein kinase termed hSLK. Subsequent analysis failed to validate the recovered clone as a true interacting protein. To allow a further characterization of the kinase, a muscle λgt11 cDNA library (Clontech) was screened to isolate full-length clones. Full-

* Corresponding author. Mailing address: MOBIX, Institute for Molecular Biology and Biotechnology, McMaster University, Life Science Bldg., Rm. 437, 1280 Main St. West, Hamilton, Ontario, Canada L8S 4K1. Phone: (905) 525-9140, ext. 27424. Fax: (905) 521-2955. E-mail: rudnicki@mcmaster.ca.

length cDNA inserts were subcloned into pBluescript and sequenced on an ABI automated sequencer. Homology searches were performed with National Center for Biotechnology Information Blast software, and homologies are presented as percent identities.

Cell culture, transfection, luciferase assays, and microinjection. C2C12 cells were maintained in Dulbecco's modified Eagle medium supplemented with 15% fetal calf serum (FCS). Rat1-Myc/ER, NIH 3T3, Swiss 3T3, and 293 cells were grown in Dulbecco's modified Eagle medium containing 10% FCS. Rat1-Myc/ER cells were induced to undergo apoptosis by the addition of 2 μM β-estradiol for the indicated period. Apoptosis in NIH 3T3 and Swiss 3T3 cells was induced by the addition of TNF-α (50 ng/ml) and 10 μM pyrrolidinedithiocarbamate (PDC). For luciferase assays and stimulation of 293, the cells were plated at 10^5/35-mm-diameter dish 24 h prior to transfection. The cultures were transfected by Lipofectamine (Gibco/BRL) according to the manufacturer's instructions, using 1 μg of Gal4-luciferase reporter, 1 μg of SLK expression vector, and 100 ng of effector plasmid. For luciferase assays, 293 cells were harvested 18 to 20 h following transfection, and the cells were lysed in reporter lysis buffer (Gibco/BRL). Equivalent portions of extracts were assayed on a Lumat-100 luminometer, using 100 μl of luciferase assay reagents (Promega). Averages of five independent experiments, performed in duplicate and normalized to protein concentration, are shown.

Northern analysis, immunofluorescence, and apoptosis assays. For expression analysis, poly(A)$^+$ RNA from various adult mouse tissues was selected through oligo (dT)-cellulose (49) and subjected to Northern blot analysis using a SLK-specific probe. Analysis of SLK protein expression was performed by lysing the cultures (150 mM NaCl, 50 mM Tris [pH 7.4], 1 mM EDTA, 1% Triton X-100, 1 mM phenylmethylsulfonyl fluoride, 1 mM dithiothreitol, 1 μg each of aprotinin, pepstatin, and leupeptin per ml; for kinase assay, the buffer was supplemented with 10 mM sodium fluoride, 10 mM β-glycerophosphate, and 1 mM sodium orthovanadate) and subjecting 20 μg of total lysate to Western blot analysis using anti-SLK rabbit polyclonal antibodies. Reactive proteins were detected by enhanced chemiluminescence (Amersham) using a goat anti-rabbit horseradish peroxidase-labeled secondary antibody. SLK polyclonal antibodies were generated by immunization of New Zealand rabbits with purified glutathione *S*-transferase (GST)–SLK$^{95–551}$ (anti-SLK1), encompassing part of the kinase and microtubule- and nucleus-associated protein (M-NAP) domains, or GST–SLK$^{1–93}$ (anti-SLK2; kinase domain). Specific immunoreactivity to murine SLK protein was observed in 293 cells transfected with full-length and truncated SLK expression vectors.

For expression studies and immunolocalization experiments, hemagglutinin or Myc epitope-tagged pcDNA3 (Invitrogen) expression vectors bearing full-length or truncated SLK were constructed by using standard cloning procedures (49). Briefly, SLK$^{1–373}$ was constructed by deleting amino acids 374 to 1202, leaving the kinase domain. The SLK$^{373\text{-}1202}$ deletion was generated by deletion of the first 372 amino acids of SLK. The kinase-dead version, SLK^{K63R}, and the cleavage mutant, SLK^{D436N}, were obtained through PCR-based mutagenesis of the ATP binding site at residue 63 and the aspartic acide at position 436, respectively. Plasmid SLK$^{1–950}$ was created by deleting the last C-terminal 263 amino acids of Myc-SLK. Plasmid SLK$^{551–950}$ encompasses amino acids 551 to 950. The expression vector SLK$^{856–1202}$ contains amino acids 856 to 1202. Finally SLK$^{950–1202}$ was generated by inserting a fragment encompassing the last 253 amino acids of SLK into Myc-tagged pcDNA3.

Following transfection into C2C12, the cultures were fixed for 10 min in 4% paraformaldehyde and SLK protein was detected by using antibody 9E10 in conjunction with fluorescein isothiocyanate (FITC)- or tetramethyl rhodamine isocyanate (TRITC)-labeled secondary antibodies. Actin stress fibers were detected with 220 nM TRITC-phalloidin (Sigma) on fixed cultures for 15 min. Cells undergoing apoptosis were detected with annexin V-FITC (Oncor) or by TUNEL (terminal deoxynucleotidyltransferase-mediated dUTP-biotin nick end labeling) staining (Oncor) according to the manufacturer's specifications.

For the detection of endogenous SLK protein, Swiss 3T3 or C2C12 cells were fixed in 4% phosphonoformic acid and stained with anti-SLK1 antibodies followed by either TRITC-phalloidin or antivinculin antibodies. The stained coverslips were subjected to confocal microscopy using a Zeiss LSM10 microscope.

Immunoprecipitations and in vitro kinase assays. Bacterially expressed GST-SLK and immunoprecipitated Myc-SLK autophosphorylated and efficiently phosphorylated myelin basic protein (MBP) and histone H1 in vitro (not shown). Therefore, all assays were performed with histone H1 or MBP. For in vitro kinase assays, 300 μg of total cell lysate was immunoprecipitated with 1 μg of monoclonal antibody 9E10 or 1 μg of anti-SLK polyclonal antibodies and 20 μl of protein G-Sepharose (Pharmacia) for 2 h at 4°C. Immunoprecipitates were washed three times with NETN (50 mM Tris-HCl [pH 7.5], 150 mM NaCl, 1 mM EDTA, 0.1% Nonidet P-40) and once with kinase assay buffer (20 mM Tris-HCl [pH 7.5], 15 mM $MgCl_2$, 10 mM NaF, 10 mM β-glycerophosphate, 1 mM sodium orthovanadate). Reactions (20 μl) were initiated by the addition of 5 μCi of [γ^{32}P]ATP and 3 μg of histone H1 or MBP. After a 30-min incubation at 30°C, reactions were terminated by the addition of 4× sodium dodecyl sulfate (SDS) sample buffer, and 20-μl aliquots were fractionated by polyacrylamide gel electrophoresis (PAGE) on SDS–12% gels. The gels were stained, dried, and exposed to X-ray films. For coupled caspase 3 cleavage/kinase assays, immunoprecipitated SLK proteins were incubated at 37°C in the presence or absence of caspase 3 lysates or purified caspase 3 (Pharmingen) and then washed extensively with NETN and subjected to kinase assays using histone H1 as described above. Caspase 3-expressing bacterial lysates or Rat1-Myc/ER lysates were prepared as described by Song et al. (52). Cleavage assays on immunoprecipitated or in vitro-labeled (Promega TNT system) SLK proteins were performed as described elsewhere (52).

Nucleotide sequence accession number. The SLK sequence shown in Fig. 1A has been assigned GenBank accession no. AF112855.

RESULTS

SLK is a member of a novel class of ubiquitously expressed Ste20-related kinases. During the course of a two-hybrid screen for interacting proteins with a muscle-specific transactivator, several putative binding proteins were isolated. One clone containing a 1.6-kb partial cDNA insert showed extensive homology to hSLK. Subsequent analysis failed to validate the recovered clone as a true interacting protein. To allow a further characterization of the murine kinase, a muscle λgt11 cDNA library (Clontech) was screened to isolate full-length clones. We recovered 5,253-bp cDNA (clone 3E5) that encoded the full-length 1,202-amino-acid polypeptide (predicted molecular mass of 147 kDa) and had over 90% nucleotide identity with human, rat, and guinea pig SLK sequences (19) recently deposited in the database.

Searches for homologous proteins revealed that the amino-terminal kinase domain was closely related to corresponding domains of the Ste20-related serine/threonine kinase LOK and *Xenopus* polo-like kinase kinase 1 (xPlkk1), involved in cell cycle control (43). Extensive alignment analysis of kinase domains between SLK and other related kinases demonstrated that SLK is highly related to LOK and xPlkk1 (74 and 72% identity, respectively) (Table 1). SLK was found to be closely related to human MST1 and -2 as well as germinal center kinase (GCK), with similarity indices of around 37% (Table 1). Our results suggest that SLK, LOK, and xPlkk1 represent members of a new kinase subgroup belonging to the SPS/GCK family of protein kinases.

In addition, the central domain of SLK was found to be highly homologous to M-NAP. The remaining carboxy-terminal region of SLK displayed high homology to the LOK carboxy terminus of xPlkk1 and AT1–46, a cDNA clone encoding a protein of unknown function (50) (Fig. 1A). These observations strongly suggest that SLK, LOK, and xPlkk1 may represent members of a new protein kinase family. Furthermore, the AT1–46 homology domain, also found in LOK and xPlkk1, might be a novel protein motif likely to be important for LOK, Plkk1, and SLK functions. We have termed this candidate motif the ATH (AT1–46 homology) domain. In addition, analysis of SLK primary sequence revealed the presence of a putative caspase 3 consensus cleavage site (DTQD^{436}) (38) at amino acid residue 436, within the M-NAP region.

Northern blotting analysis of poly(A)$^+$ RNA from various murine tissues with a SLK-specific probe revealed the existence of at least three distinct isoforms of about 6, 7, and 8 kb, with the larger isoform being the most abundant. Most tissues expressed similar levels of SLK mRNAs with the exception of liver, which displayed somewhat lower levels (data not shown).

SLK overexpression results in apoptosis. To determine the effect of SLK overexpression in cultured cells, a Myc epitope-tagged expression vector carrying full-length SLK was constructed and transfected into C2C12 myoblasts. To evaluate the cellular distribution of SLK, immunostaining was performed on fixed cells following transient transfections using monoclonal antibody 9E10, reactive to the Myc epitope. Interestingly, 9E10-positive cells displayed expression of Myc-SLK protein in distinct cytosolic domains (Fig. 2A).

Inspection of SLK-transfected cultures after 24 h revealed

TABLE 1. Similarity between mouse SLK and various other serine/threonine kinases

Kinase	Similarity index (%)[a]										
	mSLK	HLOK	xPlkk1	hMST1	hMST2	HKHS	hGCK	Hmst-3	hHPK1	ySPS1	HPAK1
mSLK		74	72	37	37	37	36	35	32	29	10
hLOK			85	39	38	38	37	37	37	32	10
xPlkk1				38	37	37	36	35	36	31	11
hMST1					90	38	38	47	37	34	10
hMST2						37	38	48	37	34	11
hKHS							67	39	64	33	11
hGCK								38	60	33	10
hmst-3									36	40	11
hHPK1										34	10
ySPS1											10
hPAK1											

[a] Obtained following alignment (Clustal method) of the kinases with the MegAlign program (DNAstar software package). Similarity indices indicate that murine (mSLK), human LOK (hLOK), and xPlkk1 represent a new subgroup of the GCK family of kinases. ySPS1, yeast SPS1.

the presence of numerous cells that exhibited extensive cellular shrinkage, membrane blebbing, and loss of substrate adhesion (Fig. 2B). Moreover, several 9E10-positive cellular fragments reminiscent of apoptotic bodies were evident following SLK transfection into C2C12 cells (Fig. 2E and F). Similar results were observed following transfection of SLK into COS-1, HeLa, and NIH 3T3 cells (not shown). Taken together, these data suggested that forced expression of SLK induced an apoptotic response.

To determine whether SLK-transfected cells were exhibiting a bona fide apoptotic response, double staining was performed with 9E10 and FITC-labeled annexin V or by TUNEL for the detection of apoptotic cells. Double-staining experiments performed 24 h following Myc-SLK transfection revealed the colocalization of FITC-annexin V and Myc-tagged SLK protein (Fig. 2C and D). Furthermore, over 75% of the cells that expressed the transfected Myc-SLK protein were found to be TUNEL positive (Fig. 2E and F). However, 48 h after transfection, virtually no SLK-expressing cells were detectable. Taken together, these results demonstrate that forced expression of SLK in C2C12 myoblasts triggered an apoptotic response.

SLK expression in vivo correlates with a reduction in focal adhesions and actin fibers. Focal adhesions are large protein complexes particularly prominent in cultured cells involved in cellular adherence to the substratum (7, 9, 20, 51). Focal adhesion complexes are enriched for proteins such as paxillin, vinculin, and focal adhesion kinase which modulate focal contact dynamics. The observation that cells overexpressing SLK retracted from the substrate and underwent apoptosis raised the possibility that SLK is involved in cytoskeletal remodeling. To address this question, Swiss 3T3 and C2C12 cells grown in 10% FCS were subjected to double immunofluorescence staining using antivinculin antibodies or TRITC-phalloidin and anti-SLK1 antibodies. Confocal analysis through stained Swiss 3T3 or C2C12 cells revealed that SLK localized to the cytosol (Fig. 3). Interestingly, colocalization of strongly staining focal adhesions and SLK protein was never observed, suggesting that SLK localizes to areas of weak cellular adherence (Fig. 3C

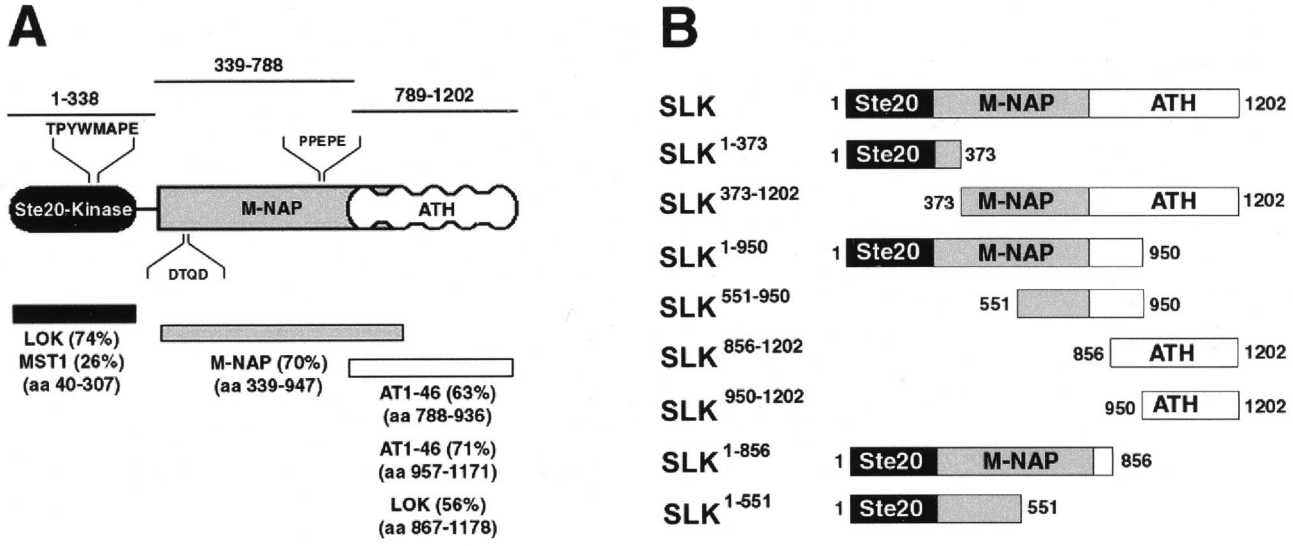

FIG. 1. Structure and expression of SLK. (A) Schematic representation of SLK and percent similarities (in parentheses) to other proteins. The catalytic domain (black) is most similar to LOK and MST1/2, two Ste20-related kinases. SLK is highly homologous to M-NAP (grey) and to AT1-46 (white) in the carboxy-terminal region. Numbers in brackets represent SLK amino acid (aa) residues. The Ste20 signature sequence (TPYWMAPE), caspase 3 consensus cleavage site (DTQD), and a putative SH3 binding domain (PPEPE) are shown. Numbers above the different domains denote the amino acid residues representing the boundaries. (B) Schematic representation of the plasmid expression vectors used in this study. The Ste20 kinase (black), M-NAP (grey), and ATH (white) domains are indicated. SLK amino acid residues are indicated at the N and C termini.

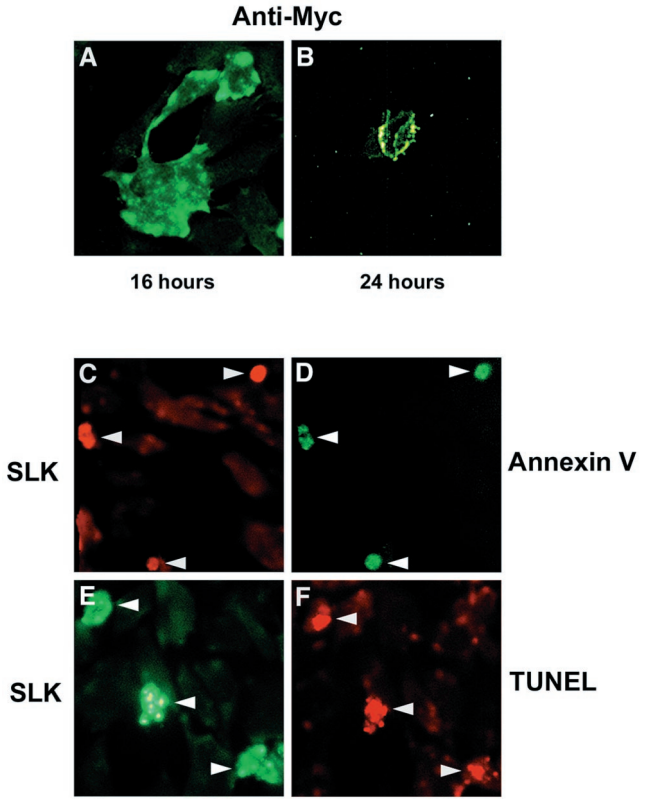

FIG. 2. Induction of apoptosis in SLK-transfected C2C12 myoblasts. (A) C2C12 cells were transiently transfected with a plasmid expressing Myc epitope-tagged SLK and at various times after transfection stained for expression with anti-Myc antibody 9E10. Distinct clusters of staining were observed at the periphery of the cells 16 h after transfection. (B) Detection of Myc-SLK 24 h following transfection revealed that 9E10-labeled cells exhibited membrane blebbing and cell shrinkage, suggesting that SLK induced cell death. (C and D) Double immunofluorescent staining of Myc-SLK and annexin V-FITC in transfected C2C12 cells, indicating that SLK transfection induces apoptosis. Arrowheads point to identical cells in panels C and D. (E and F) Immunodetection of Myc-SLK expression in cells undergoing DNA fragmentation as detected by TUNEL labeling, supporting the contention that forced expression of SLK induces apoptosis. Arrowheads mark identical cells in panels E and F.

and F). Double-labeling experiments using TRITC-phalloidin and anti-SLK1 antibodies yielded similar results (Fig. 3G to I). Interestingly, the cytoplasmic levels of SLK were found to be variable, suggesting that its expression may be regulated as cells progress through the cell cycle. Cells that displayed high levels of SLK were devoid of strongly staining stress fiber and showed actin relocalization to the periphery. However, cells expressing low levels of SLK showed a relatively high abundance of stress fibers (Fig. 3G to I), supporting the hypothesis that activated SLK induces actin reorganization to the cell periphery.

SLK overexpression induces actin stress fiber dissolution. The finding that SLK expression was correlated with a reduced number of focal adhesions and actin stress fibers suggests that SLK mediates cytoskeletal reorganization. To investigate a possible role for SLK in cellular remodeling, C2C12 cells were transfected with SLK and actin stress fibers were detected by phalloidin staining. For comparison, cells were transfected with members of the Rho family of small GTPases, which regulate the assembly of focal adhesions and stress fibers by recruiting several protein kinases through direct interaction (8, 39). Activated RhoA, which promotes stress fiber and focal complex assembly, as well as activated Rac1 and PAK3, both previously shown to induce actin stress fiber disassembly (8, 39, 56), were used as controls.

Transfected myoblasts overexpressing SLK showed almost a complete absence of stress fibers together with redistribution of actin to the cell periphery (Fig. 4A and B). This observation suggested that SLK induced stress fiber dissolution and actin reorganization. The catalytically inactive SLK mutant SLK^{K63R} also promoted stress fiber dissolution, suggesting that SLK-mediated actin reorganization is independent of kinase activity (not shown). The disassembly of stress fibers induced by SLK was comparable to that observed for the activated form of Rac1, $Rac1^{G12V}$ (Fig. 4C and D). Similarly PAK^{DE}, an activated form of PAK3, also mediated the dissolution of stress fibers in C2C12 myoblasts (Fig. 4E and F). In contrast to the observed induction of stress fiber formation in Swiss 3T3 cells (46), overexpression of activated RhoA ($RhoA^{G14V}$) in C2C12 cells similarly induced apoptosis (not shown). Taken together, these data indicate that SLK may be a potent regulator of actin fiber dynamics.

Induction of apoptosis and actin disassembly by SLK are separable activities. Several members of the SPS/GCK group of kinases have been shown to be activated by C-terminal truncation of a putative autoregulatory region (15, 42). The similarity between SLK and members of that family raised the possibility that SLK could also be activated through C-terminal deletions. To test this, several Myc-tagged truncations were generated and evaluated for kinase activity following transfection in 293 cells. In contrast to the predicted size of 147 kDa, transfected full-length SLK displayed an SDS-PAGE gel mobility of approximately 220 kDa, suggesting possible posttranslational modifications. Deletion of residues 951 to 1202 resulted in a marked increase in kinase activity, suggesting that these residues negatively regulate SLK activity (Fig. 5L). Further deletion of amino acids 857 to 950 did not lead to any further increase in kinase activity. Interestingly, deletion of residues 552 to 1202 resulted in a decrease in activity to wild-type levels compared to $SLK^{1–950}$ and $SLK^{1–856}$, suggesting that SLK activity can be autoregulated by multiple domains. Surprisingly, further deletion up to residue 373 resulted in a 10- to 15-fold increase in activity over wild-type levels (Fig. 5L). As for other SPS/GCK family members, these data strongly suggest that the carboxy-terminal region (residues 374 to 1202) contains negative autoregulatory domains that may repress kinase activity. Therefore, the $SLK^{1–373}$ truncation was then used as the activated form of SLK in subsequent assays.

The observation that the kinase-inactive SLK^{K63R} also promoted actin reorganization suggested that stress fiber dissolution by SLK was independent of kinase activity (not shown). To investigate this hypothesis, we constructed vectors expressing Myc-tagged wild-type and mutant SLK truncations and performed phalloidin staining of transfected C2C12 cells. Two of the vectors, $SLK^{1–373}$ and $SLK^{1–373}$K63R, contained the wild-type and mutant SLK kinase domain from residues 1 to 373, extending slightly into the M-NAP region, 66 residues short of the caspase cleavage site (see Fig. 5L and 1C for plasmid vectors). The wild-type form of this truncation displayed about a 10-fold increase in kinase activity compared to full-length SLK in an in vitro kinase assay (Fig. 5L).

Relative to wild-type SLK, overexpression of $SLK^{1–373}$ in C2C12 cells resulted in a markedly increased rate of apoptosis, as evidenced by a large increase in the numbers of cells exhibiting cellular shrinkage and membrane blebbing 16 h following transfection (Fig. 5A and B). To determine the effect of overexpression of the activated form $SLK^{1–373}$ on stress fiber dynamics, cultures were fixed and stained at earlier time points (12 h) following transfection. As shown in Fig. 5I and J, over-

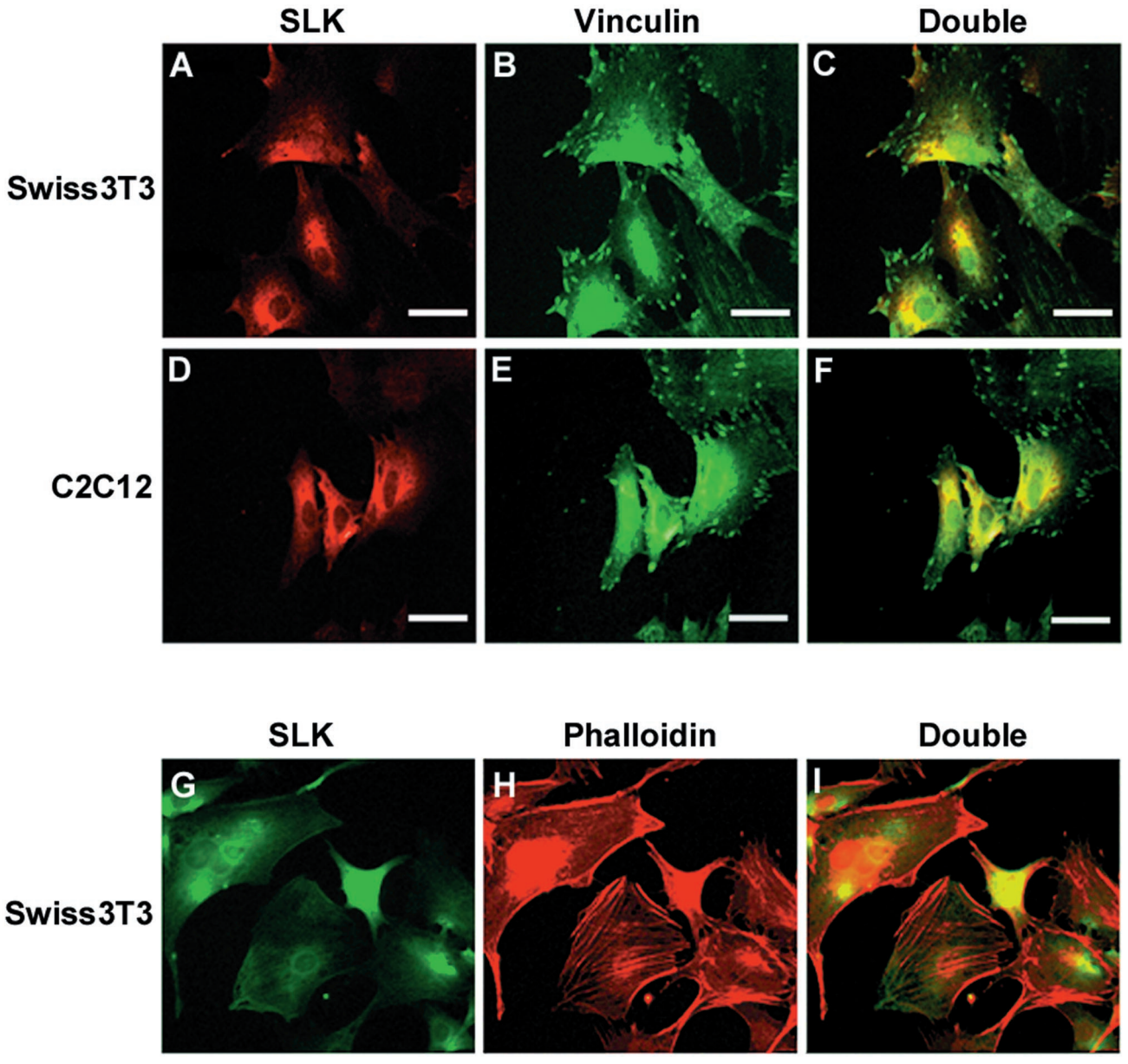

FIG. 3. Localization of endogenous SLK protein. (A and B) Immunostaining of endogenous SLK (A) and vinculin (B) in Swiss 3T3 fibroblasts. (C) Superposition of panels A and B. (D and E) Immunostaining of SLK (D) and vinculin (E) in C2C12 myoblasts. (F) Superposition of panels D and E. (G and H) Immunostaining of endogenous SLK (G) and phalloidin stain (H) of Swiss 3T3 cells. (I) Double exposure of the stained cells. In both cell types, SLK staining was found to be excluded from vinculin- and actin fiber-positive areas, supporting a role for SLK in cellular remodeling. Scale bar = 50 μm.

expression of activated SLK resulted in a rapid loss of strongly staining stress fibers and redistribution of actin to the cellular periphery, suggesting that the apoptotic response induced by activated SLK is triggered following stress fiber disassembly. In contrast, forced expression of the kinase-inactive $SLK^{1–373K63R}$ did not induce cell death (Fig. 5C), suggesting that enhanced apoptotic response is due to activation of the kinase domain. However, overexpression of $SLK^{1–373K63R}$ did not result in any apparent loss of stress fibers following transfection (Fig. 5D). Consistent with the observation that SLK-mediated actin reorganization is also independent of kinase activity, a mutant lacking the kinase domain up to residue 372 (termed $SLK^{373–1202}$ [Fig. 1C]), strongly promoted stress fiber disassembly (Fig. 5E and F). In addition, $SLK^{373–1202}$-transfected cultures contained a high proportion of retracting cells, suggesting that the SLK C-terminal domain is a potent effector of stress fiber dissolution.

To evaluate the rate of apoptosis induced by the various Myc-tagged SLK vectors, the proportion of annexin V and 9E10 double-positive cells was measured relative to the total number of 9E10-positive cells. As shown in Fig. 5K, cultures transfected with the active $SLK^{1–373}$ displayed about a sixfold increase in numbers of double-positive apoptotic cells 16 h posttransfection compared to cultures transfected with $SLK^{1–373K63R}$ or control vector. Transfection with $SLK^{373–1202}$ resulted in a frequency of double-positive apoptotic cells that was about threefold less than that observed in cultures transfected with $SLK^{1–373}$ and similar to that observed in cultures transfected with full length SLK (not shown). In summary, these results suggest that both N- and C-terminal domains of

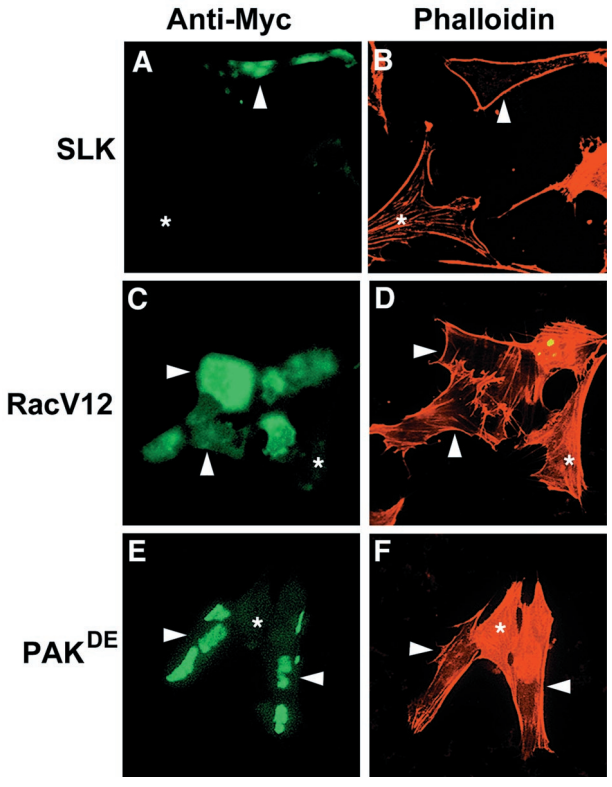

FIG. 4. Overexpression of SLK induces stress fiber dissolution. (A and B) Expression of Myc-SLK in transiently transfected C2C12 cells induced loss of actin stress fibers as detected by phalloidin staining. Arrowheads mark the same cell in panels A and B; asterisks mark an untransfected cell. (C and D) Expression of Myc-Rac^{V12} in C2C12 cells similarly induced loss of stress fibers, as evidenced by phalloidin staining. Arrowheads mark identical cells in panels C and D; asterisks indicate an untransfected cell. (E and F) Expression of transfected Myc-p65^{PAK} also induced loss of actin stress fibers. Arrowheads mark identical cells in panels E and F; asterisks indicate an untransfected cell. The cells were fixed and stained 16 h posttransfection with anti-Myc antibody 9E10 and TRITC-phalloidin and then photographed at 400×.

SLK were capable of inducing apoptosis. Forced expression of the N-terminal kinase domain resulted in a rapid and efficient induction of apoptosis that was dependent on kinase activity. By contrast, forced expression of the C-terminal actin disassembling region resulted in stress fiber dissolution followed by induction of apoptosis likely due to cellular retraction and loss of adhesion.

The ATH domain mediates actin disassembly. To further delineate the domains that mediate stress fiber disassembly, we generated a series of Myc-SLK deletions and truncations and evaluated their ability to reorganize actin stress fibers (Fig. 1C). SLK$^{1–950}$ bears a carboxy-terminal deletion of 252 amino acids, removing part of the ATH domain. Construct SLK$^{551–950}$ encompasses SLK amino acids 551 to 950, spanning part of the kinase domain extending into the M-NAP region. Construct SLK$^{856–1202}$ contains amino acids 856 to 1202, extending to the end of the ATH domain. Finally, SLK$^{950–1202}$ encodes the last C-terminal 253 amino acids of the ATH region that are deleted in SLK$^{1–950}$. Expression plasmids were transiently transfected into C2C12 cells, and the cultures were fixed and processed for Myc epitope and phalloidin staining.

Overexpression of SLK$^{1–950}$ led to a markedly increased density of actin stress fibers, suggesting that the carboxyl 253 amino acids negatively regulate actin polymerization (Table 2). Transfection of SLK$^{1–950}$ nevertheless resulted in an apoptotic response marked by shrinkage and membrane blebbing (not shown). Transfection of SLK$^{551–950}$ resulted in a perinuclear staining pattern together with an increased density of strongly staining stress fibers but did not induce apoptosis (Table 2 and data not shown). Therefore, we conclude that the ATH region of SLK is required to effect actin reorganization. Supporting this conclusion, transfection of SLK$^{856–1202}$, bearing a partial deletion of the M-NAP region but encompassing the ATH domain, efficiently effected the disassembly of actin stress fibers and thereafter induced apoptosis (Table 2).

Taken together, transfection of the various deletion constructs mapped a stress fiber-disassembling domain of SLK to the last carboxy-terminal 253 amino acids. To confirm this, SLK$^{950–1202}$ was constructed and transfected into C2C12 cells. Phalloidin staining of SLK$^{950–1202}$-expressing cells revealed a dramatic loss of actin fibers (Fig. 5G and H; Table 2). In addition, most cells expressing SLK$^{950–1202}$ displayed a morphology reminiscent of cellular retraction, suggesting that the ATH domain is sufficient to induce stress fiber dissolution and loss of substrate adherence.

Caspase 3 cleavage stimulates kinase activation. Inspection of the SLK protein sequence revealed the presence of a putative caspase 3 cleavage site, DTQD^{436} (38) at amino acid position 436. This observation, together with the findings that SLK mediated apoptosis and stress fiber disassembly through distinct domains, raised the possibility that SLK represents a novel caspase 3 substrate.

To investigate this possibility, full-length wild-type SLK and the caspase 3 cleavage site mutant SLK^{D436N} were translated in vitro in the presence of [^{35}S]methionine. The translation products were incubated with purified recombinant caspase 3, or alternatively with lysates from Rat1-Myc/ER cells triggered to undergo apoptosis (12), and then analyzed by SDS-PAGE. As shown in Fig. 6A and B, in vitro-translated SLK displayed a complex banding pattern due to the presence of incomplete translation products. Nevertheless, caspase 3 cleavage products of approximately 133 and 60 kDa were observed following incubation of SLK with purified caspase 3 or a Rat1-Myc/ER apoptotic lysate (Fig. 6A and B). Interestingly, mutation of the cleavage site at residue 436 and incubation with an apoptotic lysate resulted in a cleavage pattern that was identical to that for wild-type SLK, suggesting that SLK cleavage occurs at multiple nonconsensus sites (Fig. 6A and B). Addition of the caspase 3 inhibitor Z-DEVD-fmk inhibited the release of the fragments from wild-type SLK, indicating that cleavage is mediated by a caspase 3-like activity (Fig. 6B). Identical results were obtained following incubation of wild-type SLK or SLK^{D436N} with purified caspase 3 (Fig. 6A).

The cleavage of SLK by a caspase 3-like activity following incubation with an apoptotic cell lysate raised the possibility that SLK is an in vivo substrate for caspases during an apoptotic response. To address this, Rat1-Myc/ER cells, expressing a Myc-estrogen receptor fusion (12), were induced to undergo apoptosis by the addition of β-estradiol, and extracts were subjected to Western blot analysis using different anti-SLK polyclonal antibodies. Western analysis with anti-SLK1 antibody, directed against the kinase domain and the M-NAP region, showed anti-SLK-reactive products of approximately 220, 133, and 60 kDa. The relative amounts of the 133- and 60-kDa products were found to increase over time following the onset of Myc-induced apoptosis (Fig. 6C). In addition, reactive species of about 150 kDa were found to be estradiol sensitive and to decrease over time. Whether these are smaller SLK products or unrelated cross-reactive species remains to be determined.

Analysis of the same extracts with anti-SLK2, a kinase do-

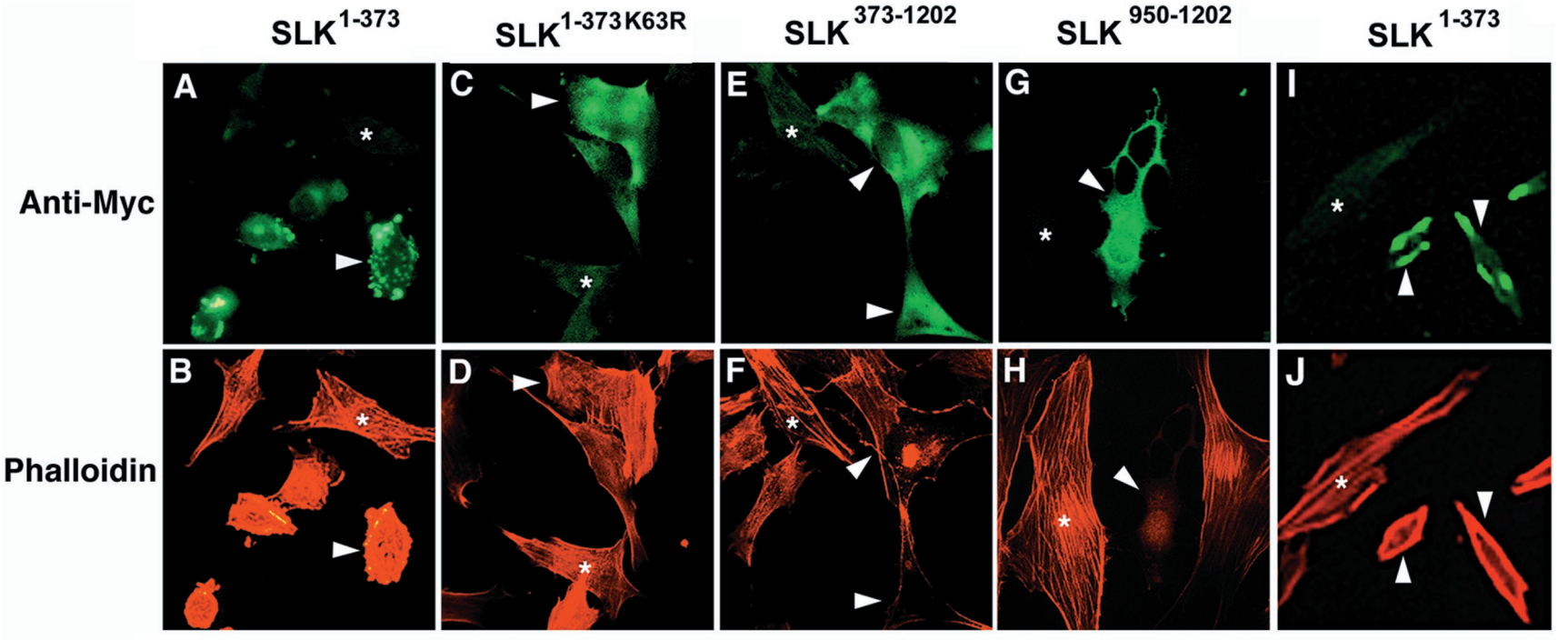
SLK 1-373
SLK 1-373K63R
SLK 373-1202
SLK 950-1202
SLK 1-373
Anti-Myc
Phalloidin
A
B
C
D
E
F
G
H
I
J

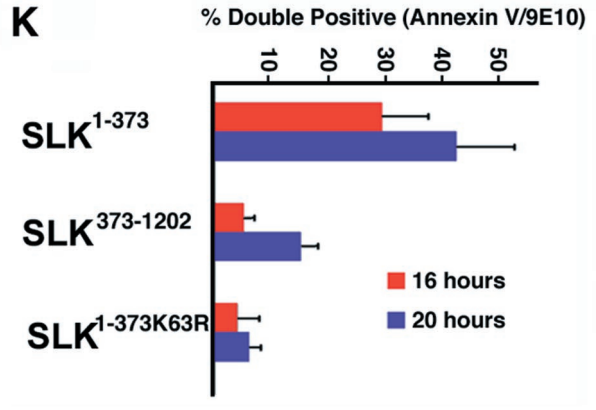
K
% Double Positive (Annexin V/9E10)
10
20
30
40
50
SLK 1-373
SLK 373-1202
SLK 1-373K63R
16 hours
20 hours

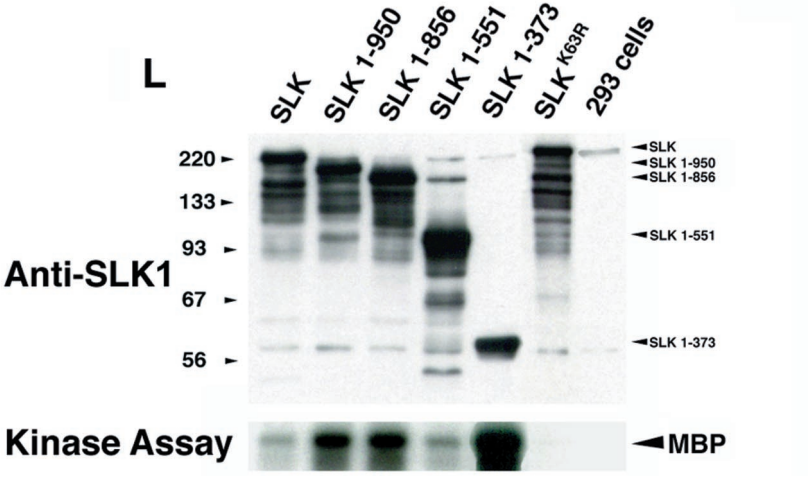
L
SLK
SLK 1-950
SLK 1-856
SLK 1-551
SLK 1-373
SLK K63R
293 cells
220
133
93
67
56
Anti-SLK1
Kinase Assay
SLK
SLK 1-950
SLK 1-856
SLK 1-551
SLK 1-373
MBP

FIG. 5. Distinct SLK domains induce apoptosis and stress fiber disassembly. (A and B) Immunodetection and phalloidin staining of Myc-$SLK^{1–373}$-expressing C2C12 cells 16 h posttransfection. Extensive membrane blebbing was observed in expressing cells. An untransfected cell is indicated by an asterisk. (C and D) Overexpression of the Myc-$SLK^{1–373K63R}$ mutant did not result in any morphological changes suggesting that it is kinase dependent. Each asterisk indicates an untransfected cell. (E and F) Forced expression of Myc-$SLK^{373–1202}$ induced stress fiber dissolution in overexpressing cells, as shown by phalloidin staining demonstrating that SLK may play important roles in the regulation of actin reorganization. An untransfected cell (asterisk) is shown for comparison. (G and H) Transfection of the AT1–46 domain ($SLK^{950–1202}$) resulted in a loss of strongly staining actin stress fibers relative to untransfected cells (asterisk), indicating that an actin-reorganizing domain of SLK is contained within the ATH region. Photomicrographs are shown at 400×. (I and J) Analysis of Myc-SLK1–373-expressing cells 12 h following transfection shows cellular shrinkage redistribution of actin to the periphery and loss of actin stress fibers. For comparison, an untransfected cell is shown (asterisk). Photomicrographs are shown at 400×. (K) Enhanced apoptotic response by $SLK^{1–373}$ overexpression. The percentage of annexin V and 9E10 double-positive cells relative to the total number of 9E10-positive cells was evaluated at 16 and 20 h following transfection. The results revealed an increased rate of cell death by $SLK^{1–373}$. (L) Identification of a C-terminal autoregulatory domain. Myc-tagged wild-type, mutant (SLK^{K63R}), and C-terminal truncation mutants $SLK^{1–950}$, $SLK^{1–856}$, $SLK^{1–551}$, and $SLK^{1–373}$ were transfected into 293T cells, immunoprecipitated with antibody 9E10, and assayed for kinase activity on MBP (arrow). As a control, kinase-dead SLK was also assayed. Equivalent aliquots of protein were also subjected to Western blot analysis for normalization using anti-SLK1 antibodies (upper panel). About a 10-fold-higher kinase activity was consistently observed with immunoprecipitated $SLK^{1–373}$.

TABLE 2. Actin disassembling and apoptosis-inducing activities of SLK mutants and N- and C-terminal truncations

Expression vector	Actin disassembly[a]	Kinase activity[b]	Apoptosis	Cellular localization[c]
SLK	+	+	+	CP
$SLK^{1–373}$	−	+++	+++	DC
$SLK^{373–1202}$	+	−	+	DC
$SLK^{1–950}$	−[d]	+	+	DC
$SLK^{551–950}$	−[d]	−	−	PN
$SLK^{856–1202}$	+	−	+	DC
$SLK^{950–1202}$	++	−	+	DC
SLK^{K63R}	+	−	+	CP

[a] Following transfection into C2C12 cells, the cultures were fixed and stained with anti-Myc and TRITC-phalloidin to evaluate their actin-disassembling activity. At least 100 transfected cells were scored for each construct.

[b] Determined by immunoprecipitations and in vitro kinase assays following transfections in 293 cells.

[c] CP, cell periphery; DC, diffuse cytoplasmic; PN, perinuclear.

[d] An increased density of stress fibers was observed following transfection of $SLK^{1–950}$ and $SLK^{551–950}$.

main-specific antibody, resulted in the detection of the 60-kDa cleavage fragment 12 h following the addition of β-estradiol (Fig. 6D, lanes 3 to 5). Anti-SLK2 antibodies did not detect the 133-kDa fragment, suggesting that it represents the C-terminal domains of SLK (not shown). Western blot analysis of caspase 3-treated N-terminal Myc-tagged SLK with antibody 9E10 also detected a 60-kDa product (data not shown). Similarly, release of a 60-kDa anti-SLK2-reactive product was observed when NIH 3T3 cells were exposed to apoptotic triggers such as TNF-α and UV irradiation (Fig. 6D, lanes 6 to 9). To determine whether SLK cleavage in vivo is mediated solely by caspase 3 or other potential interleukin-1β-converting enzyme-like proteases, MCF-7 cells lacking expression of caspase 3 were induced to undergo apoptosis using TNF-α and analyzed for SLK cleavage. As shown in Fig. 6C, no differences were observed in the pattern of anti-SLK-reactive bands before or 16 h after the addition of TNF-α to the cells, suggesting that SLK cleavage in vivo during apoptosis is mediated by caspase 3. Our results indicate that caspase 3 cleavage of SLK in vivo releases the kinase domain as an N-terminal 60-kDa product and that this cleavage represent a common step in response to various apoptotic stimuli.

To investigate the effect of caspase 3 cleavage on SLK activity, various SLK mutants were transfected into 293 cells, immunoprecipitated, and assayed for kinase activity following treatment with recombinant caspase 3 in vitro. As shown in Fig. 7A, exposure of wild-type or a truncated SLK protein ($SLK^{1–950}$) to recombinant caspase 3 resulted in a marked increase in kinase activity. Following caspase 3 treatment, the resulting kinase activity for wild-type SLK was similar to that observed for the untreated kinase domain mutant $SLK^{1–373}$. These results strongly suggest that processing of SLK by caspase 3 releases and activates the amino-terminal kinase domain. Shown in Fig. 7B is a Western blot demonstrating expression of the different SLK mutants used in the kinase assays (Fig. 7A) following tranfection into 293 cells.

Recently, second-bleed anti-SLK antisera were found to immunoprecipitate endogenous SLK from murine cell lines. Therefore, to investigate whether SLK activity is modulated in vivo during an apoptotic response, Swiss 3T3 cells were treated with TNF-α in growth medium for various periods of time, and total lysates were subjected to immunoprecipitations and kinase assays. As shown in Fig. 7C, SLK activity on MBP was found to be upregulated threefold 2 h following the addition of

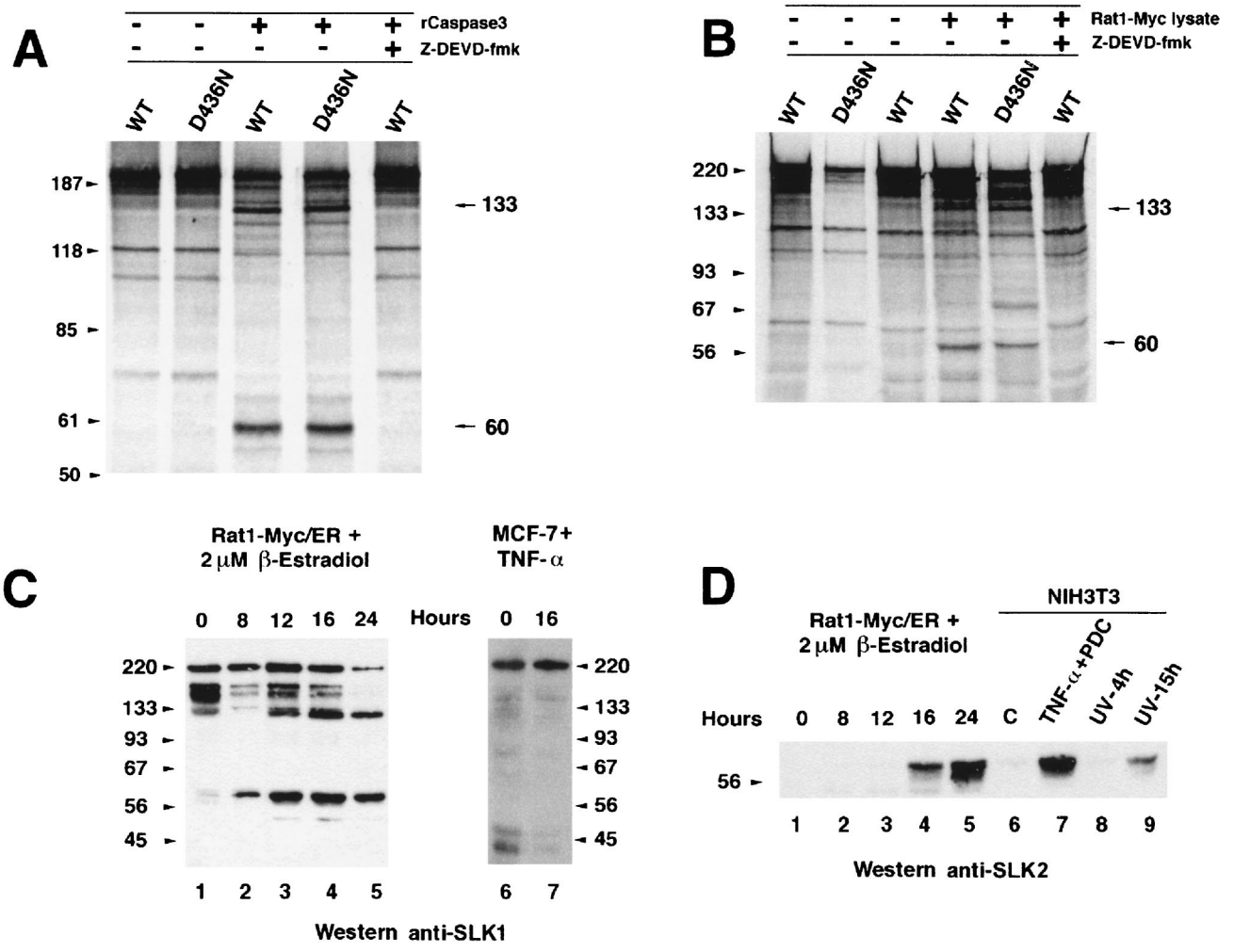

FIG. 6. Caspase 3 cleavage of in vitro-translated wild-type (WT) and caspase 3 cleavage site mutant (D436N) SLK proteins during apoptosis. (A) In vitro-translated SLK and SLK^{D436N} were incubated in the presence of purified caspase 3 and analyzed by SDS-PAGE. Caspase 3-specific cleavage products were observed for both constructs. Sizes are indicated in kilodaltons. (B) A similar pattern of cleavage was observed in the presence of an apoptotic cell lysate from induced (2 μM β-estradiol) Rat1-Myc/ER cells. Introduction of the D436N mutation in SLK did not prevent cleavage and release of cleavage products. Addition of the caspase 3 inhibitor Z-DEVD-fmk (50 μM) to the reaction abolished cleavage. (C) Apoptosis-induced cleavage of endogenous SLK protein in stimulated Rat1-Myc/ER cells. The levels of SLK fragments of 133 and 60 kDa progressively increased during the apoptotic response, while the levels of the full-length p220 and reactive 150-kDa species were reduced. (D) N-terminal-specific antibodies identified the 60-kDa fragment as the kinase domain in induced Rat1-Myc/ER cells and NIH 3T3 cells exposed to apoptotic triggers. NIH 3T3 fibroblasts were exposed to TNF-α (50 ng/ml) plus 10 μM PDC for 16 h or UV-irradiated (180 J/m^2) and allowed to recover in growth medium for 4 and 15 h. Release of the SLK kinase domain was clearly evident. No reactivity to the 133-kDa fragment was observed, suggesting that it bears a C-terminal portion of SLK.

TNF-α. The kinase activity was found to remain elevated for up to 4 h and declined below control levels at 8 h after treatment. Western blot analysis of the same extracts showed that an increase in the 60-kDa fragment correlated with the increase in kinase activity 2 h following TNF-α addition (Fig. 7C). However, even though kinase activity remained high at 4 h, the levels of the 60-kDa fragment declined below control levels, suggesting that the full-length kinase may have been activated. In contrast to Myc-induced apoptosis, the 133-kDa fragment was not detected in TNF-α-treated Swiss 3T3 cells. Instead, a new fragment of approximately 50 kDa was readily apparent 2 h after treatment (Fig. 7D), suggesting that different apoptotic trigger may lead to differential processing of SLK.

Activation of JNK by SLK overexpression. To gain insights into potential downstream effectors of SLK, plasmids expressing Gal4-Jun, Gal4-Elk1, and Gal4-CREB fusions (Pathdetect plasmid system; Stratagene) were cotransfected with a full-length wild-type SLK expression vector together with a Gal4-luciferase reporter gene. Transfection of SLK with Gal4-Jun resulted in a five- to sevenfold increase in luciferase activity relative to Gal4-Jun alone (Fig. 8). This observation suggested that SLK overexpression activated the JNK pathway. However, JNK activation by SLK overexpression was about threefold less than that observed with MEK kinase (MEKK), an upstream regulator of JNK (13). Relative to either effector transfected alone, a modest (two- to threefold) increase in reporter gene activity was observed when SLK was cotransfected with Gal4-Elk or Gal4-CREB (Fig. 8). Therefore, SLK overexpression appeared to predominantly activate the JNK pathway. Supporting this inference, in vitro kinase assays revealed that active JNK1 was readily immunoprecipitated from SLK-transfected 293 cells whereas ERK1/2 remained inactive (not shown).

To determine wether activation of JNK by SLK occurs through a known MEKK, transfections were performed in the presence of dominant negative versions of MEKK or SEK1, both upstream activators of JNK (13). Cotransfection of both dominant negative SEK1 and MEKK along with SLK and Gal4-

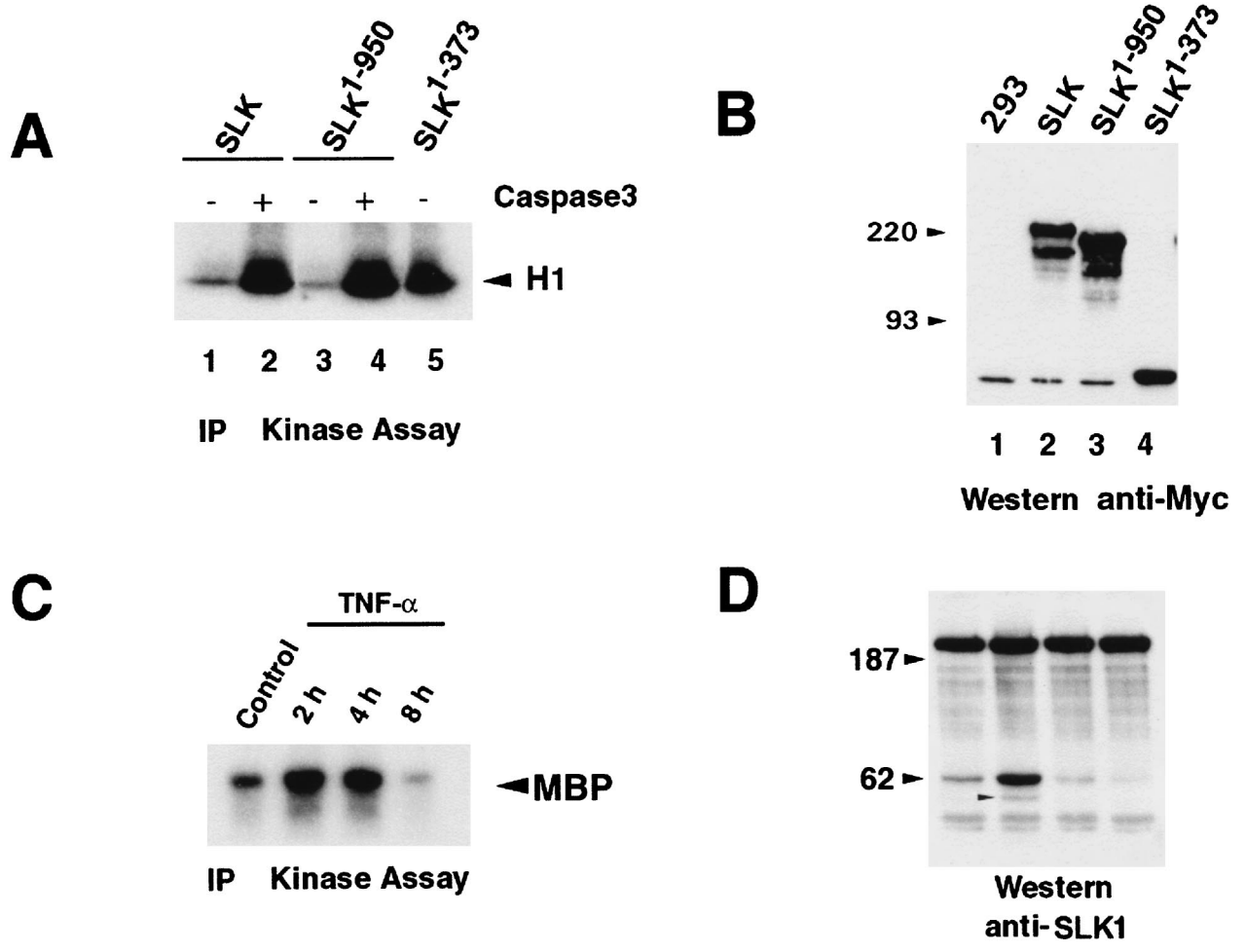

FIG. 7. Activation of SLK through caspase 3-mediated cleavage. (A) In vitro caspase 3/kinase assay on immunoprecipitated (IP) Myc-SLK proteins. Wild-type or mutant Myc-SLK proteins were immunopurified, subjected to caspase 3-expressing lysates or a control lysate, and assayed for kinase activity in vitro. (B) Anti-Myc tag Western blot analysis of immunoprecipitations performed in panel A, showing expression of all Myc-SLK proteins in transfected 293 cells. Sizes are indicated in kilodaltons. (C) In vitro kinase assay of immunoprecipitated SLK protein following TNF-α (50 ng/ml) and PDC (10 μM) treatment of subconfluent Swiss 3T3 cultures. SLK activity was found to be upregulated threefold 2 h following the addition of TNF-α. (D) Western blot analysis of TNF-α-treated Swiss 3T3 cultures (as in panel C). The increase in SLK activity was correlated with the appearance of the 60-kDa anti-SLK-reactive species and a 50-kDa product (small arrowhead).

Jun resulted in an inhibition of luciferase reporter activity, suggesting that JNK activation by SLK occurs through MEKK and SEK.

DISCUSSION

SLK, a Ste20-related kinase. We have cloned and characterized a murine protein kinase, SLK, that mediates apoptosis and actin reorganization. The cloned cDNA encodes the mouse homologue of human SLK and is highly related to xPlkk1, an activator of Plx1 essential for spindle assembly (Table 1 and reference 43, and LOK, a Ste20-related protein kinase preferentially expressed in lymphocytes (26). Whether, as for xPlkk1, SLK plays a major role in the control of the cell cycle remains to be elucidated. Analysis of the kinase domain revealed that SLK is a member of the SPS/GCK family of serine/threonine kinases and is related to MST1/2 (10, 15) and more distantly related to Ste20, a yeast kinase involved in the pheromone response pathway (63). Northern blot analysis demonstrated that SLK is ubiquitously expressed in adult tissues.

SLK induces apoptosis and stress fiber disassembly. SLK-transfected cells exhibited cellular shrinkage and membrane blebbing suggestive of programmed cell death. Staining of the transfected cultures for specific apoptotic markers such as membrane inversion and DNA fragmentation indicated that SLK rapidly induced an apoptotic response. Similarly, the recently identified but unrelated ZIP, RIP, and ASK1 kinases also induce cell death (16, 21, 53). However, truncated forms of SLK was still able to elicit an apoptotic response, suggesting that SLK could induce programmed cell death in a kinase-independent manner. This notion was confirmed by the observation that the C-terminal ATH region (lacking the kinase domain) was sufficient to induce an apoptotic response, but with delayed kinetics.

Interestingly, apoptotic membrane blebbing is regulated in part by myosin light chain (MLC) phosphorylation, and inhibitors of MLC kinase decrease membrane blebbing (34). In addition, MLC kinase activity is regulated by the Rho-binding kinase ROK (37), suggesting a role for p21-activated kinases in the process of cytoskeletal reorganization during apoptosis. Supporting this view is the observation that overexpression of

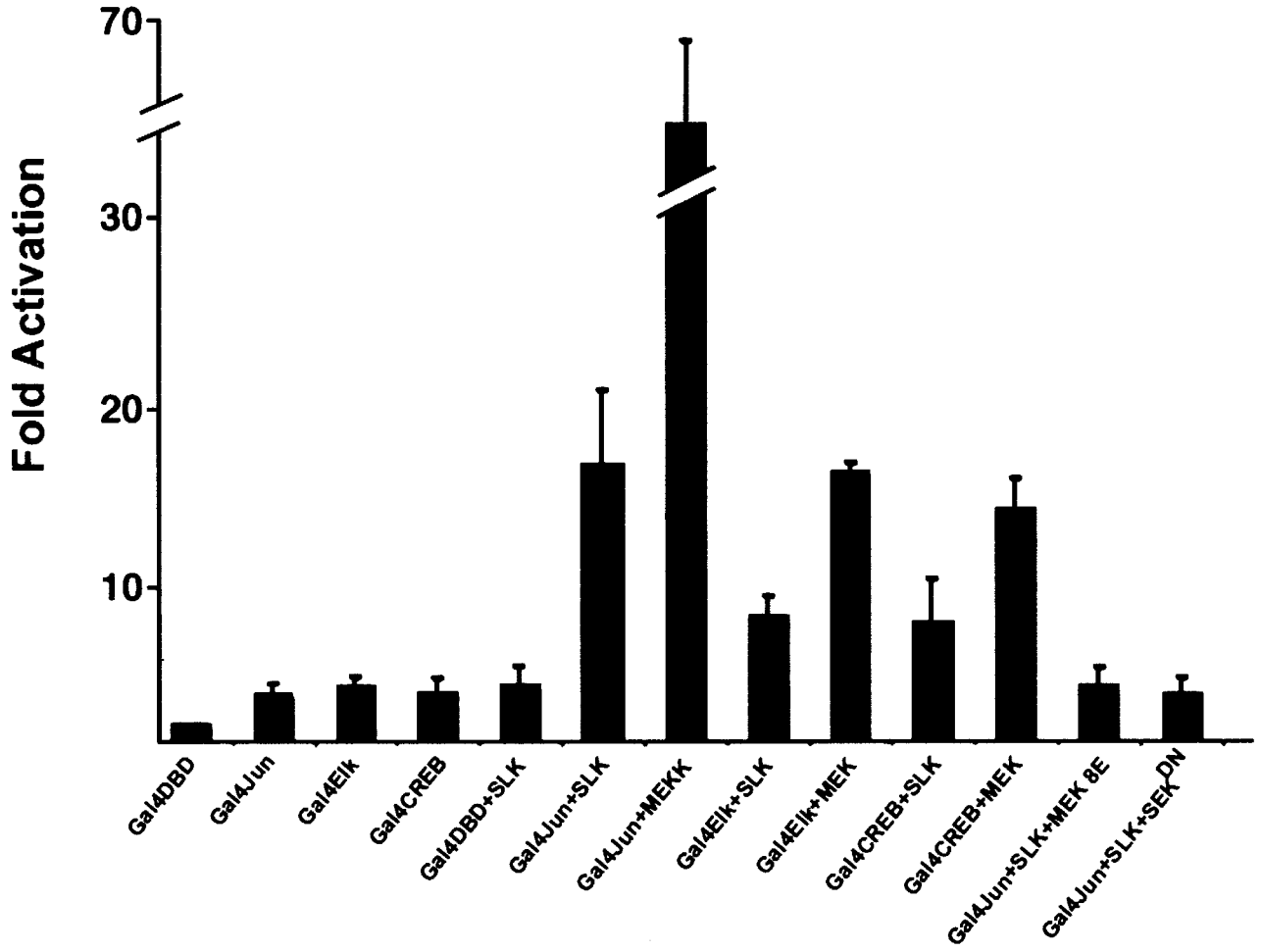

FIG. 8. SLK induces the stress-activated signaling pathway. Gal4-luciferase reporter and Gal4-Elk1, Gal4-Jun, and Gal4-CREB fusions with or without SLK were transiently transfected into 293 cells. Cotransfection of SLK and Gal4-Jun resulted in a five- to sevenfold increase in luciferase activity. By contrast, cotransfection of SLK and Gal4-Elk and Gal4-CREB resulted in a twofold increase in luciferase activity. Addition of dominant negative MEKK (MEK 8E) or SEK1 (SEK^{DN}) inhibited the SLK-mediated activation of Gal4-Jun, suggesting that SLK activates JNK through MEKK and SEK. The data shown represent averages ± standard errors from five independent experiments performed in duplicate, normalized to protein concentrations. Gal4DBD, Gal4 DNA binding domain.

$p65^{PAK}$ mutants in Fas-triggered Jurkat cells induces cell death but without the formation of apoptotic bodies (47). Extensive membrane blebbing was induced following transfection of the SLK kinase domain, and this effect was kinase dependent. Therefore, an interesting possibility is that SLK has a unique role in the regulation of cellular remodeling during programmed cell death.

Focal adhesions are dynamic protein complexes involved in cellular adherence to the substratum (9). The turnover of focal complexes and actin stress fibers is coupled to the activity of the Rho family of small GTPases (6, 17, 37). Several GTP-Rho binding proteins have been identified, including $p140^{mDia}$ and the protein kinases $p160^{ROCK}$, ROKα, MRCKα, protein kinase N, and PRK2. These GTP-Rho binding proteins appear to regulate cytoskeletal reorganization by promoting stress fiber formation (37, 56). In contrast, overexpression of α-PAK induces loss of both focal adhesions and actin stress fibers (32). Although SLK does not contain any homology to known GTPase binding domains, overexpressions of both SLK and a kinase-inactive mutant resulted in actin stress fiber dissolution, suggesting that this is a kinase-independent process. Moreover, an N-terminal deletion of SLK lacking the kinase domain efficiently promoted stress fiber disassembly and loss of focal adhesions and induced characteristic apoptotic morphology in transfected C2C12 cells. Similarly, exposure of C2C12 myoblasts to 2-chloroadenosine induces disruption of actin microfilaments and triggers apoptosis (48).

Immunolocalization and confocal analysis (1-μm slices) of endogenous SLK protein revealed that it was localized to the cytoplasm of Swiss 3T3 fibroblasts and C2C12 myoblasts. Although transfected SLK was able to induce stress fiber disassembly, immunostaining of the endogenous SLK failed to colocalize it with vinculin or paxillin at focal adhesion sites. In fact, SLK was found to localize to sites devoid of focal adhesions or stress fibers, suggesting a role for SLK in the process of cytoskeletal remodelling. Functional deletion analysis of SLK revealed that overexpression of the C-terminal ATH domain of SLK led to stress fiber dissolution and cellular retraction, suggesting that this domain negatively regulates stress fiber formation. The ATH region may interfere with regulatory components of focal complexes, supporting a role for SLK in the regulation of stress fiber dynamics.

The Ste20-related kinase PAK has been shown to be recruited to focal adhesion sites by activated Cdc42 and Rac1 (32). The presence of a putative SH3 binding domain in the M-NAP region of SLK represents an attractive target for dock-

ing onto such a protein scaffold. Whether activated p21s impinge on SLK activity is currently being investigated.

The Rho-associated kinase ROK has been shown to be implicated in the control of cytoplasmic reorganization (33) and membrane blebbing through the control of MLC kinase activity (23). Recently, ROCK and LIM-kinase have been implicated in the control of cytoskeleton reorganization through phosphorylation of cofilin, a ubiquitous actin binding protein required for actin depolymerization (3, 31, 61). Therefore, it will be of interest to identify SLK substrates. In addition, the identification of targets for the ATH domains will provide valuable clues as to the mechanisms by which SLK regulates stress fiber dynamics.

Caspase cleavage of SLK releases distinct functional domains. Although there are several kinases that mediate cell growth, only a few that trigger apoptosis have been identified. Recently, JNKs have been shown to be activated by apoptotic triggers such as Fas ligand and TNF-α (57, 60, 62). ASK1, a mitogen-activated protein (MAP) kinase kinase kinase, has been shown to induce cell death and to activate JNK and p38 MAP kinase (16). Recently, the SLK-related kinases MST1 and PAK2 have been shown to be substrates for caspase 3. Caspase-mediated cleavage was demonstrated to activate their kinase activity. In addition, MST1 has been shown to activate MKK6, MKK7, p38, and SAPKs (15). However, the mechanisms by which MST1 activates these kinases are unknown.

Similar to PAK2 and MST1 (15, 27, 28, 47), SLK is a substrate for caspase 3 and is rapidly cleaved following the induction of apoptosis. Furthermore, cleavage releases an activated kinase domain and an actin fiber-disassembling region that appear to function independently.

Several studies have demonstrated that actin fiber disassembly and cytoskeletal rearrangements represent significant steps in the process of apoptosis (5, 11, 14, 24, 35, 41, 48). Furthermore, actin has been demonstrated to be resistant to caspase cleavage during apoptosis, suggesting that it is required for cellular remodeling during the apoptotic process and that reorganization mechanisms need to be activated (45, 52, 58). Therefore, SLK may represent a novel proapoptotic effector for which caspase cleavage releases a cytoskeletal disassembling function concomitant with kinase activation. Whether the active kinase domain is involved in cytoskeletal remodeling, apoptotic signaling, or both remains to be determined.

Actin stress fibers are ultimately anchored at focal adhesion sites through interactions with proteins such as α-actinin, vinculin, and talin (9). Interestingly, overexpression of gelsolin, an actin-regulatory protein found at focal sites, has been demonstrated to protect Jurkat cells from Fas-induced apoptosis by preventing changes in the F-actin morphology and inhibition of caspase 3 (40). However, endogenous gelsolin protein was found to be a substrate for caspase 3. Caspase 3-cleaved gelsolin was demonstrated to destabilize the actin network, causing cellular retraction, detachment, and apoptosis (25). Similarly, the product of the growth arrest-specific 2 (Gas2) gene is also cleaved by an ICE-like protease activity during apoptosis (4). Gas2 is known to be associated with the actin microfilament network, and caspase cleavage induces its actin reorganization activity (4). One attractive possibility is that the caspase 3-mediated release of the ATH domain interferes directly with the function of actin-regulatory proteins such as gelsolin or Gas2 or, alternatively, may promote their proteolytic processing.

We have cloned and characterized a Ste20-related kinase, SLK, which can mediate apoptosis and promote stress fiber dissolution. Although the full-length protein can mediate both effects, the individual N- and C-terminal domains were more efficient at inducing apoptosis and actin reorganization, respectively. We have shown that SLK is a substrate for a caspase 3-like activity in vivo during the process of apoptosis. Furthermore, caspase 3-mediated cleavage of SLK increased its intrinsic kinase activity. These results raise the interesting possibility that kinases such as SLK and PAK may represent a new class of dual-function proteins playing important roles in the regulation of the apoptotic response as well as cytoskeleton reorganization. The identification of SLK substrates, regulatory molecules, and interacting partners will provide further insights into mechanisms underlying its regulation during the process of actin reorganization and programmed cell death.

ACKNOWLEDGMENTS

We thank Catherine Neville and Robert Korneluk for sequencing cDNAs, Linda Penn for kindly providing Rat1-Myc/ER cells, and Katsuyuki Tamai for raising rabbit anti-SLK antibodies. We are grateful to Sarang Kulkarni for microinjections.

L.A.S. is supported by a postdoctoral fellowship from the Medical Research Council of Canada. M.A.R. is a Research Scientist of the Medical Research Council of Canada and a member of the Genetics Disease Network of Excellence. This work was supported by a grant from the Medical Research Council of Canada to M.A.R.

REFERENCES

1. **Amano, M., K. Chihara, K. Kimura, Y. Fukata, N. Nakamura, Y. Matsuura, and K. Kaibuchi.** 1997. Formation of actin stress fibers and focal adhesions enhanced by Rho-kinase. Science **275:**1308–1311.
2. **Amano, M., H. Mukai, Y. Ono, K. Chihara, T. Matsui, Y. Hamajima, K. Okawa, A. Iwamatsu, and K. Kaibuchi.** 1996. Identification of a putative target for Rho as the serine-threonine kinase protein kinase N. Science **271:**648–650.
3. **Arber, S., F. A. Barbayannis, H. Hanser, C. Schneider, C. A. Stanyon, O. Bernard, and P. Caroni.** 1998. Regulation of actin dynamics through phosphorylation of cofilin by LIM-kinase. Nature **393:**805–809.
4. **Brancolini, C., M. Benedetti, and C. Schneider.** 1995. Microfilament reorganization during apoptosis: the role of Gas2, a possible substrate for ICE-like proteases. EMBO J. **14:**5179–5190.
5. **Brancolini, C., D. Lazarevic, J. Rodriguez, and C. Schneider.** 1997. Dismantling cell-cell contacts during apoptosis is coupled to a caspase-dependent proteolytic cleavage of beta-catenin. J. Cell Biol. **139:**759–771.
6. **Burnham, M. R., M. T. Harte, A. Richardson, J. T. Parsons, and A. H. Bouton.** 1996. The identification of p130cas-binding proteins and their role in cellular transformation. Oncogene **12:**2467–2472.
7. **Burridge, K., and M. Chrzanowska-Wodnicka.** 1996. Focal adhesions, contractility, and signaling. Annu. Rev. Cell Dev. Biol. **12:**463–518.
8. **Burridge, K., G. Nuckolls, C. Otey, F. Pavalko, K. Simon, and C. Turner.** 1990. Actin-membrane interaction in focal adhesions. Cell Differ. Dev. **32:** 337–342.
9. **Craig, S. W., and R. P. Johnson.** 1996. Assembly of focal adhesions: progress, paradigms, and portents. Curr. Opin. Cell Biol. **8:**74–85.
10. **Creasy, C. L., and J. Chernoff.** 1995. Cloning and characterization of a member of the MST subfamily of Ste20-like kinases. Gene **167:**303–306.
11. **DeMeester, S. L., J. P. Cobb, R. S. Hotchkiss, D. F. Osborne, I. E. Karl, K. W. Tinsley, and T. G. Buchman.** 1998. Stress-induced fractal rearrangement of the endothelial cell cytoskeleton causes apoptosis. Surgery **124:**362–371.
12. **Evan, G. I., A. H. Wyllie, C. S. Gilbert, T. D. Littlewood, H. Land, M. Brooks, C. M. Waters, L. Z. Penn, and D. C. Hancock.** 1992. Induction of apoptosis in fibroblasts by c-myc protein. Cell **69:**119–128.
13. **Fanger, G. R., P. Gerwins, C. Widmann, M. B. Jarpe, and G. L. Johnson.** 1997. MEKKs, GCKs, MLKs, PAKs, TAKs, and tpls: upstream regulators of the c-Jun amino-terminal kinases? Curr. Opin. Genet. Dev. **7:**67–74.
14. **Ghosh, P. M., G. E. Mott, N. Ghosh-Choudhury, R. A. Radnik, M. L. Stapleton, J. J. Ghidoni, and J. I. Kreisberg.** 1997. Lovastatin induces apoptosis by inhibiting mitotic and post-mitotic events in cultured mesangial cells. Biochim. Biophys. Acta **1359:**13–24.
15. **Graves, J. D., Y. Gotoh, K. E. Draves, D. Ambrose, D. K. Han, M. Wright, J. Chernoff, E. A. Clark, and E. G. Krebs.** 1998. Caspase-mediated activation and induction of apoptosis by the mammalian Ste20-like kinase Mst1. EMBO J. **17:**2224–2234.
16. **Ichijo, H., E. Nishida, K. Irie, P. ten Dijke, M. Saitoh, T. Moriguchi, M. Takagi, K. Matsumoto, K. Miyazono, and Y. Gotoh.** 1997. Induction of apoptosis by ASK1, a mammalian MAPKKK that activates SAPK/JNK and p38 signaling pathways. Science **275:**90–94.
17. **Ilic, D., C. H. Damsky, and T. Yamamoto.** 1997. Focal adhesion kinase: at the

crossroads of signal transduction. J. Cell Sci. **110:**401–407.
18. **Ishizaki, T., M. Naito, K. Fujisawa, M. Maekawa, N. Watanabe, Y. Saito, and S. Narumiya.** 1997. p160rock, a Rho-associated coiled-coil forming protein kinase, works downstream of Rho and induces focal adhesions. FEBS Lett. **404:**118–124.
19. **Itoh, S., Y. Kameda, E. Yamada, K. Tsujikawa, T. Mimura, and Y. Kohama.** 1997. Molecular cloning and characterization of a novel putative STE20-like kinase in guinea pigs. Arch. Biochem. Biophys. **340:**201–207.
20. **Jockusch, B. M., P. Bubeck, K. Giehl, M. Kroemker, J. Moschner, M. Rothkegel, M. Rudiger, K. Schluter, G. Stanke, and J. Winkler.** 1995. The molecular architecture of focal adhesions. Annu. Rev. Cell Dev. Biol. **11:** 379–416.
21. **Kawai, T., M. Matsumoto, K. Takeda, H. Sanjo, and S. Akira.** 1998. ZIP kinase, a novel serine/threonine kinase which mediates apoptosis. Mol. Cell. Biol. **18:**1642–1651.
22. **Kerr, J. F., A. H. Wyllie, and A. R. Currie.** 1972. Apoptosis: a basic biological phenomenon with wide-ranging implications in tissue kinetics. Br. J. Cancer **26:**239–257.
23. **Kimura, K., M. Ito, M. Amano, K. Chihara, Y. Fukata, M. Nakafuku, B. Yamamori, J. Feng, T. Nakano, K. Okawa, A. Iwamatsu, and K. Kaibuchi.** 1996. Regulation of myosin phosphatase by Rho and Rho-associated kinase (Rho-kinase). Science **273:**245–248.
24. **Kletsas, D., D. Barbieri, D. Stathakos, B. Botti, S. Bergamini, A. Tomasi, D. Monti, W. Malorni, and C. Franceschi.** 1998. The highly reducing sugar 2-deoxy-D-ribose induces apoptosis in human fibroblasts by reduced glutathione depletion and cytoskeletal disruption. Biochem. Biophys. Res. Commun. **243:**416–425.
25. **Kothakota, S., T. Azuma, C. Reinhard, A. Klippel, J. Tang, K. Chu, T. J. McGarry, M. W. Kirschner, K. Koths, D. J. Kwiatkowski, and L. T. Williams.** 1997. Caspase-3-generated fragment of gelsolin: effector of morphological change in apoptosis. Science **278:**294–298.
26. **Kuramochi, S., T. Moriguchi, K. Kuida, J. Endo, K. Semba, E. Nishida, and H. Karasuyama.** 1997. LOK is a novel mouse STE20-like protein kinase that is expressed predominantly in lymphocytes. J. Biol. Chem. **272:**22679–22684.
27. **Lee, K. K., M. Murakawa, E. Nishida, S. Tsubuki, S. Kawashima, K. Sakamaki, and S. Yonehara.** 1998. Proteolytic activation of MST/Krs, STE20-related protein kinase, by caspase during apoptosis. Oncogene **16:**3029–3037.
28. **Lee, N., H. MacDonald, C. Reinhard, R. Halenbeck, A. Roulston, T. Shi, and L. T. Williams.** 1997. Activation of hPAK65 by caspase cleavage induces some of the morphological and biochemical changes of apoptosis. Proc. Natl. Acad. Sci. USA **94:**13642–13642.
29. **Leung, T., X. Q. Chen, E. Manser, and L. Lim.** 1996. The p160 RhoA-binding kinase ROK alpha is a member of a kinase family and is involved in the reorganization of the cytoskeleton. Mol. Cell. Biol. **16:**5313–5327.
30. **Leung, T., X. Q. Chen, I. Tan, E. Manser, and L. Lim.** 1998. Myotonic dystrophy kinase-related Cdc42-binding kinase acts as a Cdc42 effector in promoting cytoskeletal reorganization. Mol. Cell. Biol. **18:**130–140.
31. **Maekawa, M., T. Ishizaki, S. Boku, N. Watanabe, A. Fujita, A. Iwamatsu, T. Obinata, K. Ohashi, K. Mizuno, and S. Narumiya.** 1999. Signaling from Rho to the actin cytoskeleton through protein kinases ROCK and LIM-kinase. Science **285:**895–898.
32. **Manser, E., H. Y. Huang, T. H. Loo, X. Q. Chen, J. M. Dong, T. Leung, and L. Lim.** 1997. Expression of constitutively active α-PAK reveals effects of the kinase on actin and focal complexes. Mol. Cell. Biol. **17:**1129–1143.
33. **Matsui, T., M. Maeda, Y. Doi, S. Yonemura, M. Amano, K. Kaibuchi, S. Tsukita, and S. Tsukita.** 1998. Rho-kinase phosphorylates COOH-terminal threonines of ezrin/radixin/moesin (ERM) proteins and regulates their head-to-tail association. J. Cell Biol. **140:**647–657.
34. **Mills, J. C., L. H. Kim, and R. N. Pittman.** 1997. Differentiation to an NGF-dependent state and apoptosis following NGF removal both occur asynchronously in cultures of PC12 cells. Exp. Cell Res. **231:**337–345.
35. **Mills, J. C., N. L. Stone, J. Erhardt, and R. N. Pittman.** 1998. Apoptotic membrane blebbing is regulated by myosin light chain phosphorylation. J. Cell Biol. **140:**627–636.
36. **Nakagawa, O., K. Fujisawa, T. Ishizaki, Y. Saito, K. Nakao, and S. Narumiya.** 1996. ROCK-I and ROCK-II, two isoforms of Rho-associated coiled-coil forming protein serine/threonine kinase in mice. FEBS Lett. **392:**189–193.
37. **Narumiya, S., T. Ishizaki, and N. Watanabe.** 1997. Rho effectors and reorganization of actin cytoskeleton. FEBS Lett. **410:**68–72.
38. **Nicholson, D. W., A. Ali, N. A. Thornberry, J. P. Vaillancourt, C. K. Ding, M. Gallant, Y. Gareau, P. R. Griffin, M. Labelle, Y. A. Lazebnik, et al.** 1995. Identification and inhibition of the ICE/CED-3 protease necessary for mammalian apoptosis. Nature **376:**37–43.
39. **Nobes, C. D., and A. Hall.** 1995. Rho, rac, and cdc42 GTPases regulate the assembly of multimolecular focal complexes associated with actin stress fibers, lamellipodia, and filopodia. Cell **81:**53–62.
40. **Ohtsu, M., N. Sakai, H. Fujita, M. Kashiwagi, S. Gasa, S. Shimizu, Y. Eguchi, Y. Tsujimoto, Y. Sakiyama, K. Kobayashi, and N. Kuzumaki.** 1997. Inhibition of apoptosis by the actin-regulatory protein gelsolin. EMBO J. **16:**4650–4656.
41. **Palladini, G., G. Finardi, and G. Bellomo.** 1996. Disruption of actin microfilament organization by cholesterol oxides in 73/73 endothelial cells. Exp. Cell Res. **223:**72–82.
42. **Pombo, C. M., J. V. Bonventre, A. Molnar, J. Kyriakis, and T. Force.** 1996. Activation of a human Ste20-like kinase by oxidant stress defines a novel stress response pathway. EMBO J. **15:**4537–4546.
43. **Qian, Y. W., E. Erikson, and J. L. Maller.** 1998. Purification and cloning of a protein kinase that phosphorylates and activates the polo-like kinase Plx1. Science **282:**1701–1704.
44. **Raff, M. C., B. A. Barres, J. F. Burne, H. S. Coles, Y. Ishizaki, and M. D. Jacobson.** 1993. Programmed cell death and the control of cell survival: lessons from the nervous system. Science **262:**695–700.
45. **Rice, R. L., D. G. Tang, and J. D. Taylor.** 1998. Actin cleavage in various tumor cells is not a critical requirement for executing apoptosis. Pathol. Oncol. Res. **4:**135–145.
46. **Ridley, A. J., and A. Hall.** 1992. The small GTP-binding protein rho regulates the assembly of focal adhesions and actin stress fibers in response to growth factors. Cell **70:**389–399.
47. **Rudel, T., and G. M. Bokoch.** 1997. Membrane and morphological changes in apoptotic cells regulated by caspase-mediated activation of PAK2. Science **276:**1571–1574.
48. **Rufini, S., G. Rainaldi, M. P. Abbracchio, C. Fiorentini, M. Capri, C. Franceschi, and W. Malorni.** 1997. Actin cytoskeleton as a target for 2-chloro adenosine: evidence for induction of apoptosis in C2C12 myoblastic cells. Biochem. Biophys. Res. Commun. **238:**361–366.
49. **Sambrook, J., E. F. Fritsch, and T. Maniatis.** 1989. Molecular cloning: a laboratory manual, 2nd ed. Cold Spring Harbor Laboratory Press, Cold Spring Harbor, N.Y.
50. **Schaar, D. G., M. R. Varia, S. Elkabes, L. Ramakrishnan, C. F. Dreyfus, and I. B. Black.** 1996. The identification of a novel cDNA preferentially expressed in the olfactory-limbic system of the adult rat. Brain Res. **721:**217–228.
51. **Schaller, M. D., and J. T. Parsons.** 1994. Focal adhesion kinase and associated proteins. Curr. Opin. Cell Biol. **6:**705–710.
52. **Song, Q., T. Wei, S. Lees-Miller, E. Alnemri, D. Watters, and M. F. Lavin.** 1997. Resistance of actin to cleavage during apoptosis. Proc. Natl. Acad. Sci. USA **94:**157–162.
53. **Stanger, B. Z., P. Leder, T. H. Lee, E. Kim, and B. Seed.** 1995. RIP: a novel protein containing a death domain that interacts with Fas/APO-1 (CD95) in yeast and causes cell death. Cell **81:**513–523.
54. **Steller, H.** 1995. Mechanisms and genes of cellular suicide. Science **267:** 1445–1449.
55. **Thornberry, N. A., and Y. Lazebnik.** 1998. Caspases: enemies within. Science **281:**1312–1316.
56. **Van Aelst, L., and C. D'Souza-Schorey.** 1997. Rho GTPases and signaling networks. Genes Dev. **11:**2295–2322.
57. **Verheij, M., R. Bose, X. H. Lin, B. Yao, W. D. Jarvis, S. Grant, M. J. Birrer, E. Szabo, L. I. Zon, J. M. Kyriakis, A. Haimovitz-Friedman, Z. Fuks, and R. N. Kolesnick.** 1996. Requirement for ceramide-initiated SAPK/JNK signalling in stress-induced apoptosis. Nature **380:**75–79.
58. **Villa, P. G., W. J. Henzel, M. Sensenbrenner, C. E. Henderson, and B. Pettmann.** 1998. Calpain inhibitors, but not caspase inhibitors, prevent actin proteolysis and DNA fragmentation during apoptosis. J. Cell Sci. **111:**713–722.
59. **Watanabe, N., P. Madaule, T. Reid, T. Ishizaki, G. Watanabe, A. Kakizuka, Y. Saito, K. Nakao, B. M. Jockusch, and S. Narumiya.** 1997. p140mDia, a mammalian homolog of Drosophila diaphanous, is a target protein for Rho small Gtpase and is a ligand for profilin. EMBO J. **16:**3044–3056.
60. **Xia, Z., M. Dickens, J. Raingeaud, R. J. Davis, and M. E. Greenberg.** 1995. Opposing effects of ERK and JNK-p38 MAP kinases on apoptosis. Science **270:**1326–1331.
61. **Yang, N., O. Higuchi, K. Ohashi, K. Nagata, A. Wada, K. Kangawa, E. Nishida, and K. Mizuno.** 1998. Cofilin phosphorylation by LIM-kinase 1 and its role in Rac-mediated actin reorganization. Nature **393:**809–812.
62. **Yang, X., R. Khosravi-Far, H. Y. Chang, and D. Baltimore.** 1997. Daxx, a novel Fas-binding protein that activates JNK and apoptosis. Cell **89:**1067–1076.
63. **Zhao, Z. S., T. Leung, E. Manser, and L. Lim.** 1995. Pheromone signalling in *Saccharomyces cerevisiae* requires the small GTP-binding protein Cdc42p and its activator CDC24. Mol. Cell. Biol. **15:**5246–5257.